23

# Formation of contrast images of specified objects by acousto-optic hyperspectrometer by selective spectral registration

© V.V. Shipko[1,2], E.A. Samoylin[1], B.E. Pozhar[2], A.S. Machikhin[2]

[1] Russian Air Force Military Educational and Scientific Center Zhukovsky?Gagarin Air Force Academy, 394064 Voronezh, Russia
[2] Scientific and Technological Center of Unique Instrumentation Russian Academy of Sciences, 117342 Moscow, Russia

e-mail: shipko.v@bk.ru

*Received 2022*
*Revised 2022*
*Accepted 2022*

The method of selecting the most informative spectral channels when using an acousto-optic hyperspectrometer in the mode of selective spectral registration is presented. The developed technique makes it possible to select spectral channels in which the maximum contrast of objects is observed against a certain background, provided that their spectral properties are known. The results of experimental studies of the technique confirm an increase in contrast compared with panchromatic and hyperspectral shooting modes in the entire optical range. The choice of spectral channels according to the presented technique can also be used both for the formation of transmission functions in a multi-window acousto-optic hyperspectrometer, and for the rapid formation of their high-contrast color-synthesized images.

**Keywords:** hyperspectral images, spectral contrast, visualization, acousto-optical filter, spectral density of energy brightness.

DOI: 10.21883/EOS.2022.10.54874.3873-22

## Introduction

Lately an intensive development of the remote-sensing instrument towards engineering of hyperspectral (HS) systems is observed. Modern samples of hyperspectral equipment cover the visible and infrared spectral ranges with the formation of hundreds of spectral-zonal images with a spectral resolution of a few nanometers [1,2]. Processing of HS images allows deciphering and recognizing objects based on the analysis of their spectra. However, in a number of problems, information about the spectra may not be enough. In this case, the HS images are visualized, which makes it possible to use spatial features in deciphering. Considering sequentially all spectral images is a labor-intensive and inefficient problem. Basically, this problem is solved at the stage of post-processing of an already formed HS image by synthesizing a new image, for example, based on the method of selecting principal components [3] or visualization by some measures of similarity with the reference sample [4] . The method [5] has also become widespread, in which a set of spectral-zonal halftone images is converted into a single image in pseudocolor. To do this, three channels are selected from the entire set of spectral channels and, representing the data, respectively, in the form of red, green and blue components, an RGB- image (a color image in natural colors) is obtained. Since this method does not use any - or additional information, one can influence the visualization result by choosing one or another coloring option. There are many options for such coloring. Most of the considered methods use the full volume of the generated HS image and require significant computational and time resources, which limits their use in real-time monitoring tasks.

Experimental studies of the information content of various HS images show that the most valuable information for various thematic tasks is concentrated, as a rule, in several spectral channels [6,7]. This circumstance provides a basis for reducing the array of information used to distinguish between objects of known spectral composition. When processing HS images, in order to save time and computational operations, it is desirable to select the most informative spectral channels in advance. Moreover, this must be done in conditions of limited computing resources, which is the case on small-sized unmanned aerial vehicles.

This approach is especially effective in the case when the registration of HS data is carried out using software-tunable optical filters i.e.acousto-optical (AO) ones [2]. These filters use dynamic diffraction gratings excited by an acoustic ultrasonic wave and are capable of performing spectral filtering of light beams without significant distortion of the images, which they carry. In this case, it is possible to reduce not only the volume of processed information, but also the volume of recorded data. This makes it possible to drastically reduce the registration time required to perform the task of distinguishing (recognizing) data. The reduction is the ratio of the total number of recorded spectral channels of the device to the number of informative channels ($N_{\text{gen}}/N_{\text{inf}}$) and can reach 2-x for typical AO filters by orders [8]. This approach is especially effective in the

analysis of line spectra with a high degree of sparseness (sparse spectra), which is typical, for example, for gas analysis problems [9,10]. In problems of observing the underlying surface, however, the spectra are continuous, which, on the one hand, does not allow automatic selection of informative points, and, on the other hand, creates conditions under which the elimination of a homogeneous or smooth component of the spectrum („background") significantly increases the image contrast.

The purpose of choosing the most informative spectral channels in the tasks of processing and analyzing HS images of objects with known spectral characteristics is to significantly speed up and simplify the procedure for obtaining HS data, as a result of which it is possible to obtain a certain set of images that provides a solution to the set thematic problem (detection and recognition of objects of different classes) with a fairly high quality score.

There are many different algorithms and methods for choosing the most informative spectral channels from the totality of all spectral channels of the HS image [6,7,11], while many of them evaluate the information content for objects of certain classes without taking into account the background, which can be quite close by spectral composition to the object. In this case, the object and its background can be classified as a single signature. At the same time, an important task of operational monitoring is the visualization of the targeted objects with high contrast in order to effectively detect and recognize them.

Implementation of selective spectral recording [12] in HS mapping is feasible using tunable AO filters. Some modern AO filters implement new functions, such as spectral window width control or spectral filtering multi-window mode [13], which could also be used to increase contrast, but these possibilities are not considered in this work. The idea of selective spectral registration, also called fragmentary spectral registration [10], is described in general terms [14] and was analyzed either under special assumptions [12] , or without registration of spatial distributions in the papers [8,10]. Thus, it is of interest to determine the approach to the optimal choice of a limited number of zones (lines) for recording the spectra of various objects for problems of contrast „visualization" of objects against various backgrounds. In this case, we will assume that the classes of the desired objects and backgrounds and their spectral characteristics are defined and known.

## Basis of method

Here, the operating principle of the AO hyperspectrometer and the algorithm for selecting spectral channels are described. The device is based on spectral narrow-band filtering of optical radiation in an AO filter (Fig. 1, *a*). The *1* camera lens forms a light beam that transfers the object image to the input of the AO filter. The linearly polarized spectral component of the incident light $\mathbf{k}_i$ separated by the input polarizer *2*, which satisfies the Bragg diffraction condition $\mathbf{k}_d = \mathbf{k}_i + \mathbf{q}$ [15], diffracts on a traveling acoustic wave $\mathbf{q}$ in an AO cell *3* with a change in the plane of linear light polarization to orthogonal ($o \to e$ or $e \to o$) and a slight deviation in the direction of propagation ($\mathbf{k}_i \to \mathbf{k}_d$). Undiffracted radiation is delayed by the output polarizer *4* crossed with the input polarizer, and the diffracted radiation is focused by the lens *5* onto the matrix photodetector *6*. The wavelength $\lambda$ of the latter is determined by the frequency $f$ of the high-frequency signal, which is applied to the piezoelectric transducer of the AO filter and creates a dynamic volumetric diffraction grating in it.

In this work, wide-aperture AO filter based on a $TeO_2$ crystal cell with a cut in the plane $(1\bar{1}0)$ was used. The cut angle is 7°. The dependence of the wavelength $\lambda$ selected by it on the ultrasound frequency $f$ is shown in Fig. 1, *b*.

To select the most informative spectral channels for hyperspectrometers based on AO filters, a priori information about the spectrum of the desired object is required. For example, the emission spectra of objects and the background, expressed in units of the spectral density of radiance, can be used as this. In this case, the brightness values are represented in $k$-bit digital form $L_n^\alpha \in [0, \ldots, 2^k - 1]$ on a set of wavelengths $\lambda$, $n = 1, \ldots, N$ is spectral channel number, $\alpha$ is symbol characterizing the object (o) or background (b) number This information in the form of a list of generated reference spectral signatures must be obtained at a preliminary stage and, if necessary, corrected during the mapping. Since it is necessary to obtain the maximum contrast image of the desired object against a certain background, it is natural to use the modulus of the difference between the spectral density of the energy brightness of the object and the background at each $n$-th wavelength $G_n = |L_n^a sacriterionfortheirdistinguishabilityo - L_n^b|$. Then the methodology for selecting the most informative spectral channels will consist of the following steps.

**Step 1.** Selecting a pair of spectra: object $L_n^o$ and background $L_n^b$. Calculation for all wavelengths of the absolute value of the difference between the values of the spectral brightness of the spectra $G_n$ of the object and the background and determining the arrays of local maxima $\lambda_m$ $(m = 1, \ldots, M)$ of the function $G_n$.

**Step 2.** Determination of the complete set of all local maxima $\lambda_m$ by enumeration of all pairwise combinations $L_n^o$ and $L_n^b$.

**Step 3.** Selection from this set of the most informative wavelengths $\lambda_p$ $(p = 1, \ldots, P)$ by the criterion $G_p \geq \varepsilon$, where $\varepsilon$ is specified threshold value chosen from the condition that each pair of object and background spectra be represented by at least one wavelength.

An alternative variant provides for the selection in each pair of spectra of the object and the background of a certain small number of informative lines and the formation of the final set from them, that is, the permutation of steps 2 and 3. Depending on this, the lines will be common for the entire class or individual for each object/background pair.

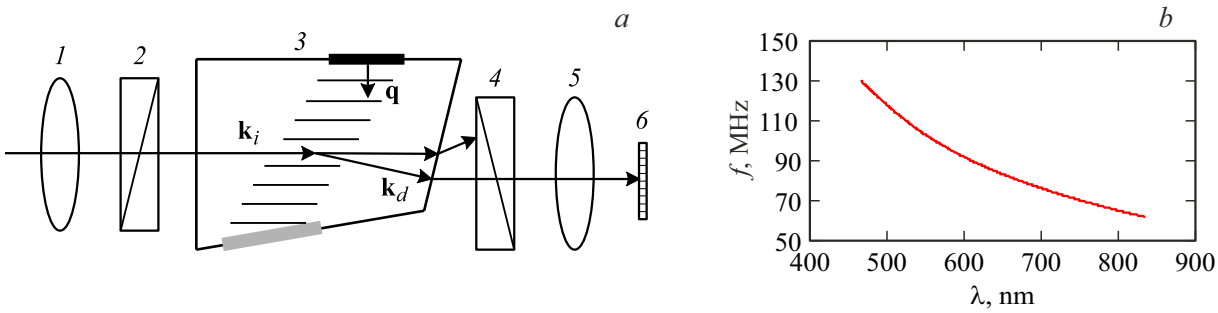


**Figure 1.** AOF scheme (*a*) and its tuning curve (*b*).

**Step 4.** The set of informative spectral points $\lambda_p$ formed for objects and backgrounds is used depending on the task to form (successively or simultaneously) $P$ frequency signals of the high-frequency generator $f_p$ to tune the AO filter to the selected wavelengths $\lambda_p$.

This method allows you to get several images (or one „polychromatic“ in multi-window mode [13]) corresponding to the highest contrast values of the object against the background from the selected classes. Physical effects that can complicate the implementation of the method are possible errors in the spectral addressing of the AO filter caused by its thermal heating and the corresponding shift in the tuning characteristic, and variations in the shape of the spectra of objects and backgrounds associated with the observation conditions. The influence of these factors will be considered in a separate work.

## Experimental implementation

To study the proposed methodology for the formation of contrast grayscale and color images using the most informative spectral channels, an experimental setup was assembled (Fig. 2).

The main equipment includes a halogen lamp%, % providing illumination of the test area of the order of 11000 lx, with a power of 150 W acoustooptical hyperspectrometer developed at the Scientific and Technological Center of Unique Instrumentation of the Russian Academy of Sciences, designed to register spectral images in the range of 450−850 nm, diffraction spectrometer used to obtain reference spectra of in the visible range with high wavelength resolution (in the 450−850 nm range), the computer with specialized software.

Testing was carried out within the framework of the task of detecting camouflage fabric against a natural background: meadow grass and sandy soil. Spectral brightness coefficients $r_n$ of objects and backgrounds obtained by a high-resolution diffraction spectrometer are shown in Fig. 3, which were calculated as the ratio of the spectral brightness of the object/background being photographed $L_n^\alpha$ to the spectral brightness, % of an equally evenly illuminated white matte surface.

In accordance with the methodology described above, the first step was to form for each object/background pair an array of spectral points $\lambda_m$, obtained by measurements of a diffraction spectrometer of % high resolution. The number of points in the array depends on the scale of the search for local maxima, and for the test samples under study, a scale of 60 spectral points turned out to be quite acceptable (Fig. 4). From the obtained estimates of local maxima for each object/background pair, three spectral channels $\lambda_p$ ($p = 1, 2, 3$) corresponding to the largest values $G_n$ were chosen. It was at these wavelengths that AO measurements were carried out with a hyperspectrometer and spectral images $L_{i,j,p}$ were obtained, where $i$, $j$ is indexes of lines and columns of the image. In addition, a total monochrome (gray halftone) image $L_{i,j,\Sigma p} = \frac{1}{3}\sum_{p=1}^{3} L_{i,j,p}$ and three-component color image $L_{i,j}^{rgb} = [L_{i,j,p=1}\, L_{i,j,p=2}\, L_{i,j,p=3}]^{\mathrm{T}}$.

Evaluation of the information content of the resulting images $L_{i,j,p}$ and $L_{i,j,\Sigma p}$ were compared with the panchromatic image $L_{i,j,\Sigma n} = N^{-1}\sum_{n=1}^{N} L_{i,j,n}$ obtained in the wavelength range $\lambda_n = 450{-}850$ nm When evaluating the object and background spectra $L_n^\alpha = \frac{1}{S^\alpha}\sum_{i,j\in S^\alpha} L_{i,j,n}^\alpha$ averaged over the regions of space $S^\alpha$ occupied by them, were used As a criterion for monochrome (gray halftone) images, the contrast ratio [16] was used, which was calculated both for the totality of all $N$ spectral components and selected $P$ (the most informative), and for each $p = 1, 2, 3$ of the spectral component separately. The greater the difference, the greater the coefficient, which depends only on the set of wavelengths used in the scene analysis. For example, for a panchromatic image, this coefficient is

$$K_1 = \frac{\left|\left(N^{-1}\sum_n L_n^{\mathrm{o}}\right) - \left(N^{-1}\sum_n L_n^{\mathrm{b}}\right)\right|}{\max\left(\left(N^{-1}\sum_n L_n^{\mathrm{o}}\right), \left(N^{-1}\sum_n L_n^{\mathrm{b}}\right)\right)} = \frac{|L_{\Sigma n}^{\mathrm{o}} - L_{\Sigma n}^{\mathrm{b}}|}{\max(L_{\Sigma n}^{\mathrm{o}}, L_{\Sigma n}^{\mathrm{b}})}. \quad (1)$$

To evaluate the information content of a color-synthesized image $L_{i,j}^{rgb}$ in three selected most informative channels in

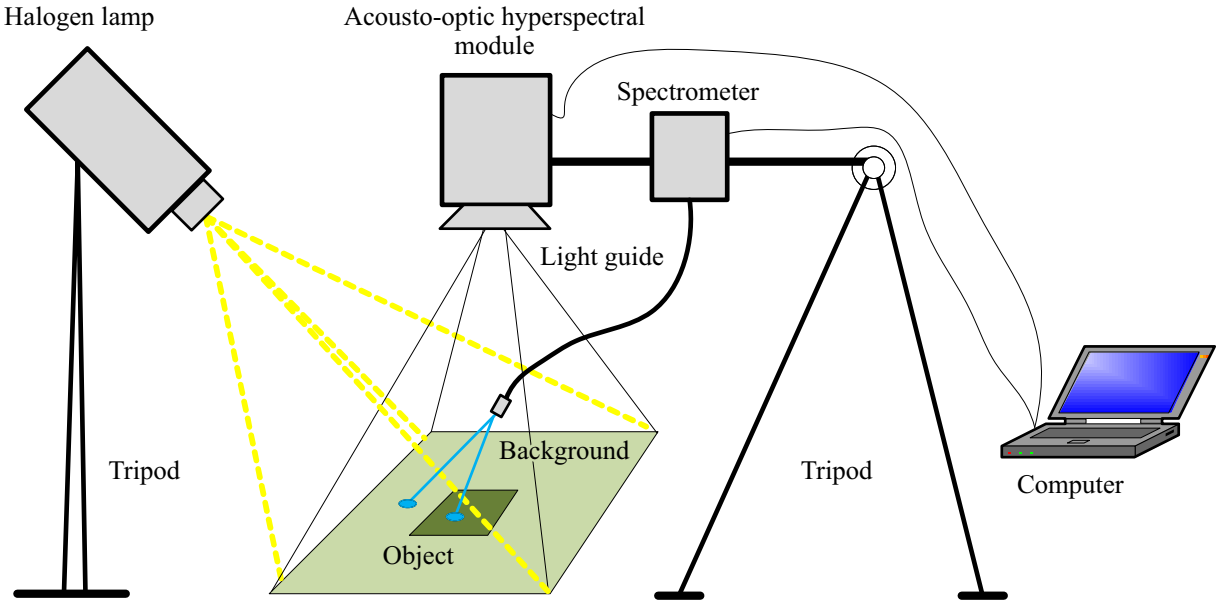


**Figure 2.** Experimental scheme.

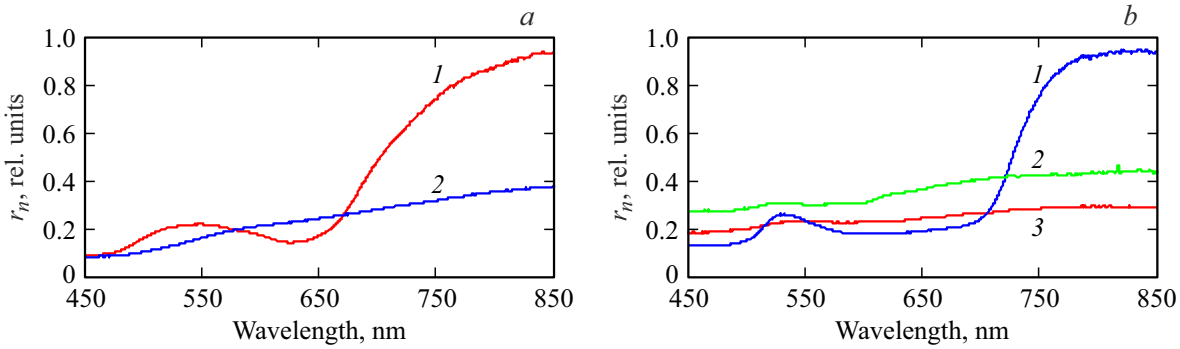


**Figure 3.** (*a*) Spectra of backgrounds (*1* is meadow grass, *2* is sand) and (*b*) objects imitating them (*1–3* is camouflage kits).

comparison with a color image in natural colors $L_{i,j}^{RGB}$ and with a GS image $L_{i,j,n}$ containing all % ($n = 73$) spectral channels, the color contrast coefficient $K_2$ [16,17] is chosen. For example, for the HS image, this coefficient has the form

$$K_2 = \frac{\sum\limits_n |L_n^{\text{o}} - L_n^{\text{b}}|}{\sum\limits_n \max(L_n^{\text{o}}, L_n^{\text{b}})}. \qquad (2)$$

Thus, $K_2$ makes it possible to take into account the contrast of each spectral component, and not the average one, as $K_1$, while $K_1$ and $K_2$ will match when the spectral curves of the object and background do not intersect and will have different values if the spectral curves intersect.

Table 1 shows the synthesized images and their corresponding contrast values (1) and (2). The results are presented as an image of a rectangle (object) on a uniform background. The amount of contrast is characterized by the visual difference between the object and the background.

Table 2 shows the frequencies of ultrasound and the corresponding wavelengths, which are selected by the AO filter during the formation of the most contrasting spectral images $L_{i,j,p}$

It can be seen from Table 1 that in all cases the values of contrast (1) for images $L_{i,j,\Sigma p}$ in the most informative spectral channels exceed the values for panchromatic images $L_{i,j,\Sigma n}$, while spectral images $L_{i,j,p}$ taken separately can provide even greater contrast. The decrease in contrast $L_{i,j,\Sigma p}$ with respect to $L_{i,j,p}$ is characterized by the fact that individual components $L_{i,j,p}$ may have inverted brightness object and background in the spectral channels $\lambda_p$ (for example, in the table $L_{p=1}$ and $L_{p=2}$ for object 2 against background 1, which have a high contrast, but inverted brightness), and when they are averaged, the contrast is equalized. Color synthesized images $L_{i,j}^{rgb}$ plotted using the most informative spectral channels give a higher color contrast (2) than RGB-images $L_{i,j}^{RGB}$ and even than the HE of the image $L_{i,j,n}$. For RGB- images, inverted brightnesses in individual spectral channels do not play a significant role

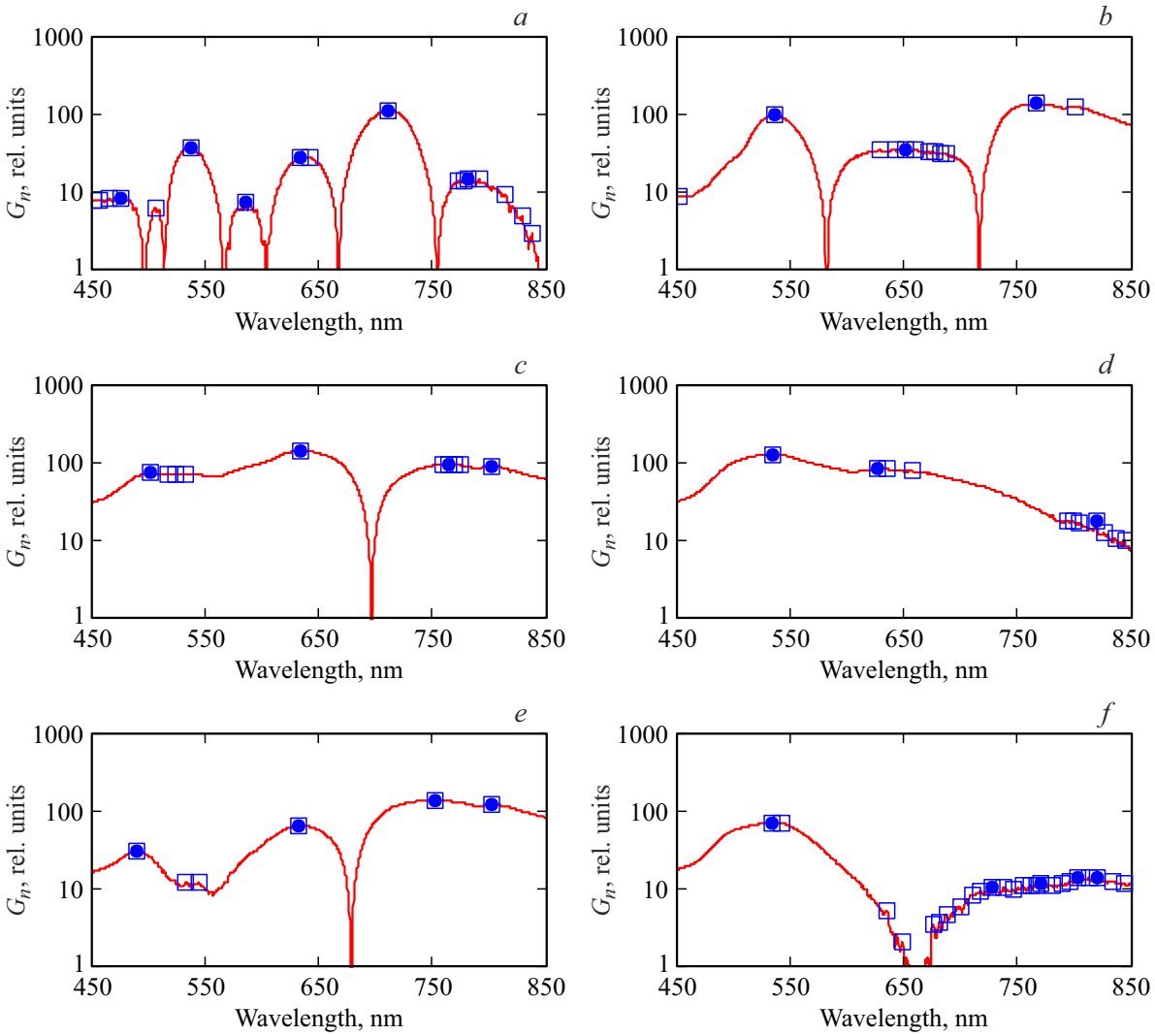


**Figure 4.** Formation of arrays of spectral points for different object/background pairs with a capture window of 30 points (squares) and 60 points (circles): *a* is object 1 on background 1, *b* is object 1 on background 2, *c* is object 2 on background 1, *d* is object 2 on background 2, *e* is object 3 on background 1, *f* is object 3 on background 2.

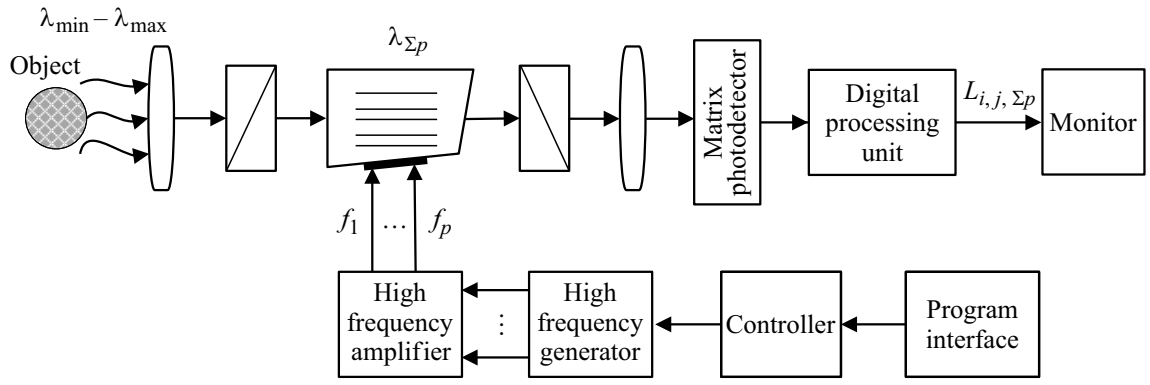


**Figure 5.** Structural diagram of a multi-window acoustooptic contrast visualization system.

and only affect the color gamut of the image. It should be noted that the main advantage of an RGB- image is the additional ability to convey the differences between an object and the background in terms of color shades, which is especially important when analyzing images by image interpreter (by human).

**Table 1.** Synthesized images of a conditional object and background and their contrast values

| Индекс объекта/фона | Наименование изображений | | | | | | | |
|---|---|---|---|---|---|---|---|---|
| | $L_{i,j,p=1}$ | $L_{i,j,p=2}$ | $L_{i,j,p=3}$ | $L_{i,j,\Sigma p}$ | $L_{i,j,\Sigma n}$ | $L_{i,j}^{rgb}$ | $L_{i,j}^{RGB}$ | $L_{i,j,n}$ |
| 1/1 | $K_1 = 0.187$ | $K_1 = 0.215$ | $K_1 = 0.497$ | $K_1 = 0.090$ | $K_1 = 0.032$ | $K_2 = 0.317$ | $K_2 = 0.151$ | $K_2 = 0.131$ |
| 1/2 | $K_1 = 0.470$ | $K_1 = 0.201$ | $K_1 = 0.605$ | $K_1 = 0.358$ | $K_1 = 0.299$ | $K_2 = 0.448$ | $K_2 = 0.339$ | $K_2 = 0.388$ |
| 2/1 | $K_1 = 0.578$ | $K_1 = 0.457$ | $K_1 = 0.509$ | $K_1 = 0.095$ | $K_1 = 0.069$ | $K_2 = 0.518$ | $K_2 = 0.357$ | $K_2 = 0.417$ |
| 2/2 | $K_1 = 0.562$ | $K_1 = 0.343$ | $K_1 = 0.343$ | $K_1 = 0.430$ | $K_1 = 0.369$ | $K_2 = 0.430$ | $K_2 = 0.258$ | $K_2 = 0.369$ |
| 3/1 | $K_1 = 0.384$ | $K_1 = 0.602$ | $K_1 = 0.658$ | $K_1 = 0.375$ | $K_1 = 0.249$ | $K_2 = 0.556$ | $K_2 = 0.090$ | $K_2 = 0.413$ |
| 3/2 | $K_1 = 0.413$ | $K_1 = 0.149$ | $K_1 = 0.194$ | $K_1 = 0.148$ | $K_1 = 0.089$ | $K_2 = 0.303$ | $K_2 = 0.237$ | $K_2 = 0.183$ |

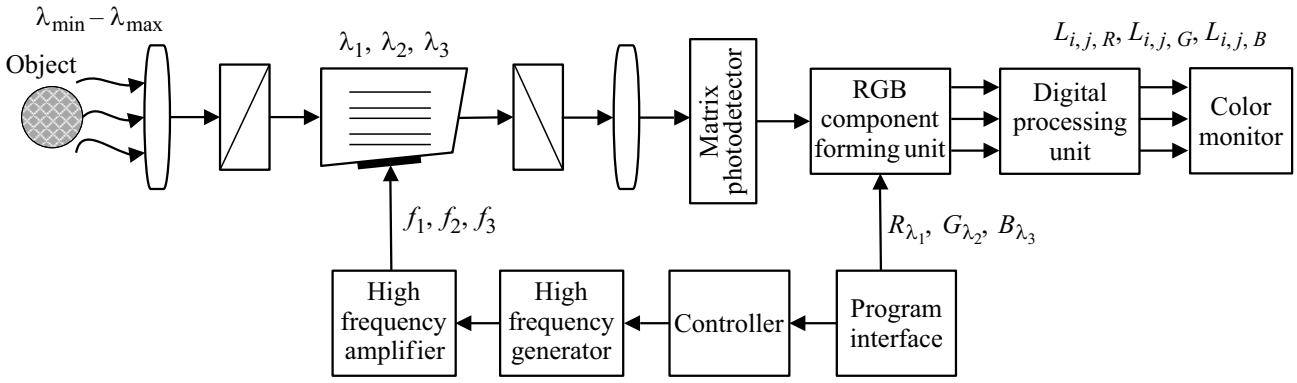


**Figure 6.** Structural diagram of an acoustooptic system for color contrast visualization.

**Table 2.** Ultrasound frequencies $f$ (MHz) and their corresponding wavelengths $\lambda$ (nm) during imaging of each object/background pair

| Index of object/ background | Frequencies of ultrasound MHz | | | Wavelengths, nm | | |
|---|---|---|---|---|---|---|
| | $f_{p=1}$ | $f_{p=2}$ | $f_{p=3}$ | $\lambda_{p=1}$ | $\lambda_{p=2}$ | $\lambda_{p=3}$ |
| 1/1 | 106.47 | 86.20 | 75.02 | 537.03 | 632.09 | 710.54 |
| 1/2 | 106.72 | 83.12 | 68.58 | 536.10 | 651.47 | 766.84 |
| 2/1 | 86.05 | 68.78 | 65.03 | 633.01 | 764.10 | 801.92 |
| 2/2 | 107.24 | 87.13 | 63.27 | 534.26 | 626.55 | 820.38 |
| 3/1 | 86.20 | 70.17 | 65.03 | 632.09 | 752.08 | 801.92 |
| 3/2 | 107.24 | 64.85 | 63.27 | 534.26 | 803.76 | 820.38 |

Gain in contrast can be defined as the ratio of the contrast of the formed image (halftone or color-synthesized) to the contrast of the original (halftone panchromatic or color in natural colors). For halftone generated images of the given set of classes „object/background“ the gain in contrast enhancement is from 15% to 8 times, for color is from 12% to 6 times.

## Structure of AO systems of selective spectral recording

Fig. 5, 6 show generalized block diagrams of AO systems that implement multi-window (Fig. 5) and color contrast imaging (Fig. 6) modes for the most informative spectral channels. Processing of registered images is carried out using the image analysis and processing unit through a software interface, which also provides general system control by setting the operating mode and parameters of the AO monochromator. The matrix photodetector in the color rendering scheme is single-channel, and the formation of color components is carried out in the corresponding block according to commands to assign a color coordinate R, G or B to a given wavelength for display on a color monitor.

## Conclusions

Thus, the results of an experimental study of the proposed approach to the choice of spectral channels confirm the possibility of increasing the contrast of given objects in comparison with panchromatic and HS imaging modes. The spectral channels selected by the presented method can be used both for the classical monitoring mode, in which one (in this case, the most informative spectral component) is singled out, and for the fast (hopping) spectral tuning mode, which allows you to quickly register several spectral components (for example, for formation of their color-synthesized images), as well as for the multi-window mode of AO contrast visualization of given objects (in which the image is formed automatically by weighted summation of individual spectral components).

All this demonstrates the validity and promise of the developed approach to the implementation of the mode of selective spectral recording of the AO hyperspectrometer, based on the choice of the most informative spectral channels when registering a set of objects with known spectral characteristics against a known set of backgrounds.

### Funding

The study was supported within the framework of the State Assignment of the .Research and Engineering Center of the Unique Devices of the RAS (project FFNS-2022-0010).

### Conflict of interest

The authors declare that they have no conflict of interest.

## References

[1] A.N. Vinogradov, V.V. Egorov, A.P. Kalinin, A.I. Rodionov, I.D. Rodionov. Opticheskiy Zhurnal, **88** (88), 4 (54) (in Russian)

[2] V.E. Pozhar, A.S. Machikhin, M.I. Gaponov, S.V. Shirokov, M.M. Mazur, A.E. Sheryshev. Svetotekhnika, **4**, 47 (2018) (in Russian). [V.E. Pozhar, A.S. Machikhin, M.I. Gaponov, S.V. Shirokov, M.M. Mazur, A.E. Sheryshev. Light & Engineering, **27** (3), 99 (2019). DOI: 10.33383/2018-029].

[3] A. Del Agila, D.S. Efremenko, T. Trautman Svetotekhnika, **4**, 60 (2019) (in Russian).

[4] T.A. Sheremetyeva, G.N. Filippov, A.M. Malov. Opticheskiy zhurnal, **82** (1), 32 (2015). [T.A. Sheremetieva, G.N. Filippov, A.M. Malov. J. Opt. Tech., **82** (1), 24 (2015)].

[5] H. Know, S.Z. Der, N.M. Nasrabadi. Opt. Eng., **41** (1), 69 (2002).

[6] S.M. Borzov, O.I. Potaturkin. Avtometriya, **56** (4), 134 (2020) (in Russian). DOI: 10.15372/AUT20200414 [S.M. Borzov, O.I. Potaturkin. Optoelectronics, Instrumentation and Data Processing, **56** (4), 431 (2020). DOI: 10.3103/S8756699020040032]

[7] I.A. Kozinov, G.N. Maltsev. Opt. i spektr., **121** (6), 1005 (2016) (in Russian). DOI: 10.7868/S0030403416120151 [I.A. Kozinov, G.N. Maltsev. Opt. Spectrosc., **121** (6), 934 (2016). DOI: 10.1134/S0030400X16120158].

[8] A.V. Fadeev, V.E. Pozhar. Opticheskiy Zhurnal,**80** (7), 50 (2013) (in Russian) [A.V. Fadeev, V.E. Pozhar. Journal of optical technology., **80** (7), 444 (2013).]

[9] M.M. Mazur, V.N. Shorin, V.I. Pustovoit, V.E. Pozhar, A.V. Fadeev. Pribory i tekhnika eksperimenta, **54**, 2 (140) (in Russian).

[10] A.V. Fadeyev, V.E. Pozhar, V.I. Pustovoit. Proc. SPIE, V. 8890, 88900H, 2013.

[11] M.A.Popov, S.A. Stankevich. Mironov, Sovremennye problemy distantsionnogo zondirovaniya Zemli iz kosmosa, **3** (106), 2006 (in Russian).

[12] V.E. Pozhar, D.Yu. Velikovskii. Opt. i spektr., **128** (7), 1035 (2020) (in Russian).
DOI: 10.21883/OS.2020.07.49578.107-20 [V.E. Pozhar, D.Y. Velikovskii. Opt. Spectrosc., **128** (7) 1041 (2020). DOI: 10.1134/S0030400X20070176].
[13] M.M. Mazur, Yu.A. Suddenok, V.E. Pozhar. Opt. i spektr., **128** (2), 284 (2020) (in Russian).
DOI: 10.21883/OS.2020.02.48980.21119 [M.M. Mazur, Y.A. Suddenok, V.E. Pozhar. Opt. Spectrosc., **128** (2) 274 (2020). DOI: 10.1134/S0030400X20020162].
[14] V.E. Pozhar, V.I. Pustovoit. Elektromagnitnyye volny i elektronnyye sistemy, **2** (4), 26 (1997) (in Russian).
[15] V.I. Balakshiy, V.N. Parygin, L.Ye. Chirkov. *Fizicheskiye osnovy akustooptiki.* (Radio i svyaz, Moskva, 1985) (in Russian). Yu.S. Sagdullayev, S.D. Kovin. *Vospriyatiye i analiz raznospektral'nykh izobrazheniy* (Sputnik+, Moskva, 2016) (in Russian).
[17] C.M. Ogreb, M.V. Tishaninov, P.M. Yukhno. Optika atmosfery i okeana, **31** (2), 160 (2018) (in Russian).
DOI: 10.15372/AOO20180213